JOURNAL OF MAGNETIC RESONANCE **124,** 355–365 (1997)
ARTICLE NO. MN961036

Systematic Errors Associated with the CPMG Pulse Sequence and Their Effect on Motional Analysis of Biomolecules

A. ROSS,* M. CZISCH,† AND G. C. KING

School of Biochemistry and Molecular Genetics, University of New South Wales, Sydney 2052, New South Wales, Australia; and †Bijvoet Center for Biomolecular Research, Utrecht University, Utrecht, The Netherlands

Received June 24, 1996; revised October 11, 1996

A theoretical approach to calculate the time evolution of magnetization during a CPMG pulse sequence of arbitrary parameter settings is developed and verified by experiment. The analysis reveals that off-resonance effects can cause systematic reductions in measured peak amplitudes that commonly lie in the range 5–25%, reaching 50% in unfavorable circumstances. These errors, which are finely dependent upon frequency offset and CPMG parameter settings, are subsequently transferred into erroneous T_2 values obtained by curve fitting, where they are reduced or amplified depending upon the magnitude of the relaxation time. Subsequent transfer to Lipari–Szabo model analysis can produce significant errors in derived motional parameters, with τ_e internal correlation times being affected somewhat more than S^2 order parameters. A hazard of this off-resonance phenomenon is its oscillatory nature, so that strongly affected and unaffected signals can be found at various frequencies within a CPMG spectrum. Methods for the reduction of the systematic error are discussed. Relaxation studies on biomolecules, especially at high field strengths, should take account of potential off-resonance contributions.

INTRODUCTION

The past few years have seen a great increase in the use of heteronuclear relaxation measurements to monitor the local motional properties of biomolecules (*1–3*). Most studies of this kind have involved the measurement of longitudinal (T_1) and transverse (T_2) relaxation times together with heteronuclear NOEs, followed by a fit of these data to one or more motional models, notably the ''model-free'' formalism developed by Lipari and Szabo (*4*). In this formalism, motions are described by a global correlation time τ_m and a local correlation time τ_e with an associated order parameter S^2 that quantifies the restriction of the local mobility. Unsatisfactory fits to the basic Lipari–Szabo formalism have been observed in numerous cases, prompting investigators to adopt extended models in order to improve the quality of fit for the divergent signals. One extended approach uses an additional correlation time describing motion on a time scale that is intermediate between the overall and internal correlation times (*5, 6*). Other authors have postulated a ''breathing'' motion of the molecule caused by conformational flexibility, with the related chemical-shift fluctuations making a selective contribution to T_2 relaxation (*7*). In a third approach, deviations from the simple model have been interpreted in terms of anisotropic molecular tumbling (*8*). The common feature of each of these extended treatments is that poor fits to the basic formalism are primarily caused by T_2 data, leading us to question the extent to which such deviations must be caused by genuine molecular motions or whether another property of the T_2 experiment may be responsible in some cases. In this context, we note that all error analysis of relaxation data conducted to date has been based solely on spectral imperfections due to thermal noise (*9*), ignoring the potential for systematic errors.

The Carr–Purcell–Meiboom–Gill (CPMG) pulse sequence (*10*) given by 90°_y —$(\Delta$—180°_x — $\Delta)_{2n}$ is the most widely used method for measuring transverse relaxation times. A detailed analysis of the effect of pulse imperfections on the behavior of this sequence was published recently (*11*). In this paper, we show that for perfect calibrated pulses the performance of the CPMG sequence is strongly dependent on its two basic experimental parameters: the pulse length and the length of the interpulse delay Δ. The influence of the delay Δ has previously been discussed in terms of the production of antiphase magnetization in coupled spin systems, where the relaxation rate of the antiphase component created during Δ differs from the relaxation rate of the desired in-phase magnetization, causing a distortion of the apparent transverse relaxation rate. This effect has been used to make recommendations concerning the maximum length of the delay period Δ (*12*). Alternatively, it has been suggested that these difficulties can be avoided by employing a spin-lock technique to measure the rotating frame relaxation time $T_{1\rho}$ (*12, 13*). In addition to these considerations, periodic inversion of the scalar-coupled spin during Δ has

* Current address: F. Hoffmann-LaRoche AG, Postfach CH-4070, Basel, Switzerland.

1090-7807/97 $25.00

been used to remove effects caused by the cross correlation of dipolar and CSA relaxation processes (*14*).

We show here that, beyond the effects mentioned above, serious reductions of experimental signal amplitudes can be caused by the off-resonance effects of the 180° pulses within the CPMG sequence. Adjustment of the length of Δ can compensate to only a limited extent. Being strongly dependent on frequency offset, the off-resonance effect may cause a subset of signals to display large and systematic errors in apparent transverse decay rates. These errors may then mislead investigators into introducing additional motional parameters into otherwise adequate models. Estimates of the systematic error based on realistic experimental hardware configurations are discussed.

THEORY

Numerical simulations of CPMG pulse sequence behavior were performed using the Bloch equations (*15*). A description based on product operators (*16*) was also employed to achieve more insight into the time evolution of the density matrix $\boldsymbol{\rho}$. All calculations were carried out for a simple one-spin system. The effect of scalar coupling has already been evaluated (*10*) and was ignored along with relaxation effects and the inhomogeneity of the B_1 field for simplicity.

For the CPMG sequence, the simplest (referred to as ''reduced'') block of pulses and delays from which the state of the system can be deduced after any arbitrary number of repetitions is given by $\Delta - 180^\circ_x - \Delta$. The time evolution of the spin system in this block can be constructed by employing a sequence of five unitary transformations: (I) a rotation U_z about the z axis caused by chemical-shift evolution during the delay Δ, (II) tilting of the reference frame by a rotation U_y about the y axis that corresponds to the off-resonance effect of the pulse, (III) rotation $U_{z'}$ about the ''new'' z axis (referred to as z') given by the flip angle of the pulse, (IV) tilting back to the normal reference frame by a rotation around the y axis, and (V) precession about the z axis during the second delay Δ. Descriptions of the angles of these rotations are given in the literature (*17*). The transformation to describe a CPMG sequence employing $2n$ repetitions of all rotations can be written using unitary transformations as

$$\begin{aligned}
\boldsymbol{\rho}_n &= (\mathbf{U}^+)^{2n}\boldsymbol{\rho}_0(\mathbf{U})^{2n}\\
\mathbf{U} &= U_z U_{-y} U_{z'} U_y U_z\\
U_z &\equiv \exp(+i2\pi f_{\mathrm{off}}\Delta I_z)\\
U_y &\equiv \exp[+i\Theta(f_1, f_{\mathrm{off}})I_y]\\
U_{z'} &\equiv \exp[+i\Phi(f_1, f_{\mathrm{off}})I_z], \qquad [1]
\end{aligned}$$

where f_{off} refers to the frequency offset from the carrier, f_1 to the field strength of the pulse in hertz, and Δ to the length of the delay in seconds. The angles Θ and Φ for a 180° pulse can be calculated according to (*17*) as

$$\Theta(f_1, f_{\mathrm{off}}) = \arctan\left(\frac{f_1}{f_{\mathrm{off}}}\right)$$

$$\Phi(f_1, f_{\mathrm{off}}) = \pi\sqrt{1 + \left(\frac{f_{\mathrm{off}}}{f_1}\right)^2}. \qquad [2]$$

To solve Eq. [1] analytically, an effective Hamiltonian related to an effective field must be constructed for a single repetition of the ''reduced'' block ($n = \frac{1}{2}$). This operator can be diagonalized by tilting the frame of reference to the axis of the effective field so calculated.

It is known that a sequence of rotations can be described by a single rotation employing an effective angle α_{eff} with respect to an effective axis $\mathbf{n}_{\mathrm{eff}}$. The orientation of this axis and its associated angle can be calculated based on the formalism of quaternions (*18*) which has been applied to the analysis of composite pulses by Counsell and co-workers (*19*). The axis $\mathbf{n}_{\mathrm{eff}}$ of two succeeding rotations of angles Φ_1 and Φ_2 around two axes given by $\mathbf{n}_1$ and $\mathbf{n}_2$ respectively can be calculated according to

$$\mathbf{n}_{\mathrm{eff}} = (s_1 c_2 \mathbf{n}_1 + c_1 s_2 \mathbf{n}_2 - s_1 s_2 \mathbf{n}_1 \times \mathbf{n}_2)/s_{\mathrm{eff}}. \qquad [3]$$

The cosine of the angle $\alpha_{\mathrm{eff}}/2$ is given by

$$c_{\mathrm{eff}} = c_1 c_2 - s_1 s_2 \mathbf{n}_1 \mathbf{n}_2, \qquad [4]$$

where c_i and s_i correspond to $\cos(\Phi_i/2)$ and $\sin(\Phi_i/2)$ respectively.

The effective axis of Eq. [1] can be calculated by repetitive application of Eqs. [3] and [4]. The result can be simplified by a symmetry argument similar to that made by Counsell *et al.* (*19*). By inserting the unity operator expressed as $\exp(-i\pi I_y)\exp(+i\pi I_y)$, it is readily shown that the inverse of the transformation given in Eq. [1] can be calculated by

$$\mathbf{U}^{-1} = \exp(+i\pi I_y)\mathbf{U}\exp(-i\pi I_y). \qquad [5]$$

Therefore, the effective rotation axis is located in the xz plane (*19*) and diagonalization of the effective Hamiltonian can be performed by tilting the frame of reference by an angle $\Theta_{\mathrm{eff}}(f_{\mathrm{off}}, f_1, \Delta)$ with respect to the y axis (Fig. 1). It should be noted that the symmetry of Eq. [5] breaks if all pulses are not applied with the same phase. To complete the transformation sequence, a rotation about the z axis by an angle $\Phi_{\mathrm{eff}}(f_{\mathrm{off}}, f_1, \Delta)$ is followed by a back-tilt in the normal reference frame resulting in

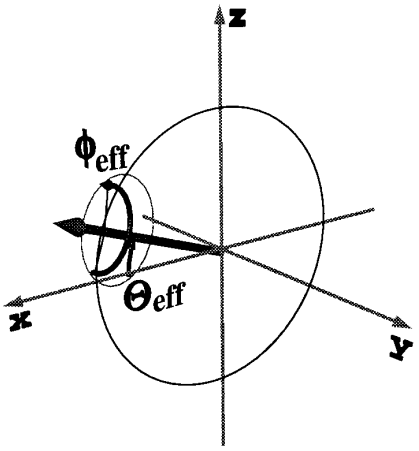

FIG. 1. Schematic of the effective rotation by the reduced block of the CPMG pulse sequence given in Eq. [7]. The angle $\Theta_{\mathrm{eff}}(x, y)$ describes the tilt angle of the effective field indicated by the bold arrow, and $\Phi_{\mathrm{eff}}(x, y)$ refers to the angle of precession about this field. The figure shows the result for an odd number of repetitions of the reduced block for emphasis. At reasonable offsets and for even numbers of repetitions, the magnetization ends up close to the x axis.

$$\begin{aligned}\mathbf{U} = &\exp[+i\Theta_{\mathrm{eff}}(f_{\mathrm{off}}, f_1, \Delta)I_y]\\ &\times \exp[-i\Phi_{\mathrm{eff}}(f_{\mathrm{off}}, f_1, \Delta)I_z]\\ &\times \exp[-i\Theta_{\mathrm{eff}}(f_{\mathrm{off}}, f_1, \Delta)I_y]. \qquad [6]\end{aligned}$$

The utility of this concept is evident for transformations where the same sequence of rotations is applied in a repetitive manner. The whole transformation for a arbitrary number of repetitions of the reduced block is given by a rotation about the same effective axis as determined by the procedure outlined above. The only effect of the repetition is that the effective angle Φ_{eff} must be multiplied by the number of cycles. The behavior of the whole CPMG experiment can thus be evaluated by that of the reduced block $(\Delta - 180^\circ_x - \Delta)$. A CPMG experiment with $2n$ repetitions of this block thus corresponds to a rotation by an angle $(2n\Phi_{\mathrm{eff}})$ about the effective axis in the xz plane:

$$\begin{aligned}\mathbf{U}_{\mathrm{CPMG}} \equiv \mathbf{U}^{2n} = &\exp[+i\Theta_{\mathrm{eff}}(f_{\mathrm{off}}, f_1, \Delta)I_y]\\ &\times \exp[-i(2n)\Phi_{\mathrm{eff}}(f_{\mathrm{off}}, f_1, \Delta)I_z]\\ &\times \exp[-i\Theta_{\mathrm{eff}}(f_{\mathrm{off}}, f_1, \Delta)I_y]. \qquad [7]\end{aligned}$$

The final state $\boldsymbol{\rho}_n = (\mathbf{U}^{+}_{\mathrm{CPMG}})\boldsymbol{\rho}_0(\mathbf{U}_{\mathrm{CPMG}})$ corresponds to magnetization with components in any direction I_x, I_y, and I_z which can be calculated from the corresponding traces of the density matrix. The I_y component results in an offset-dependent antiphase contribution to the signal while the I_z component causes loss of transverse magnetization.

For each additional repetition of the CPMG block, the magnetization ''jumps'' forward along a cycle by the angle $2\Phi_{\mathrm{eff}}$, with the center of the cycle given by Θ_{eff}. All components therefore show an oscillatory behavior with respect to the number of repetitions, so that the experimental decay curve measured with a CPMG pulse sequence can be subdivided into an exponentially decaying (zero-frequency) contribution and an oscillating amplitude. The frequency and size of the oscillating contribution is dependent on the settings of the pulse sequence parameters and the frequency offset of the signal of interest. Iterative application of Eqs. [3] and [4] for the analytical calculation of the parameters $\Theta_{\mathrm{eff}}(f_{\mathrm{off}}, f_1, \Delta)$ and $\Phi_{\mathrm{eff}}(f_{\mathrm{off}}, f_1, \Delta)$ was performed using a routine written in the Mathematica (*20*) language (available from the authors on request). The result is

$$\begin{aligned}\cos\left(\frac{\Phi_{\mathrm{eff}}}{2}\right) = &\cos(2\pi f_{\mathrm{off}}\Delta)\cos\left[\frac{\pi}{2}\left(1+\left(\frac{f_{\mathrm{off}}}{f_1}\right)^2\right)^{1/2}\right]\\ &- \sin(2\pi f_{\mathrm{off}}\Delta)\frac{\sin\left\{\frac{\pi}{2}\left[1+\left(\frac{f_{\mathrm{off}}}{f_1}\right)^2\right]^{1/2}\right\}}{\left[1+\left(\frac{f_1}{f_{\mathrm{off}}}\right)^2\right]^{1/2}}\\ \tan(\Theta_{\mathrm{eff}}) = &\sin(2\pi f_{\mathrm{off}}\Delta)\cot\left\{\frac{\pi}{2}\left[1+\left(\frac{f_{\mathrm{off}}}{f_1}\right)^2\right]^{1/2}\right\}\\ &\times\left[1+\left(\frac{f_{\mathrm{off}}}{f_1}\right)^2\right]^{1/2}\\ &+ \cos(2\pi f_{\mathrm{off}}\Delta)\frac{f_{\mathrm{off}}}{f_1}. \qquad [8]\end{aligned}$$

The same result was achieved numerically by multiplying $2n$ times the five matrices given by the unitary transformations of Eq. [1]. Further simplification was achieved with the use of normalized coordinates given by

$$x \equiv \Delta f_{\mathrm{off}} \quad y \equiv \frac{f_{\mathrm{off}}}{f_1}. \qquad [9]$$

The effect of a CPMG sequence with arbitrary parameters $(f_1, \Delta, f_{\mathrm{off}})$ on the precession angle $\Phi_{\mathrm{eff}}(x, y)$ and the effective tilt angle $\Theta_{\mathrm{eff}}(x, y)$ can be summarized in two-dimensional plots, as shown in Fig. 2A. The peak amplitude error $\delta(x, y, n)$ introduced into the measurement by the off-resonance effect can be readily determined by calculating the contribution pointing along the direction of the initial magnetization I_x via $\mathrm{Tr}(I_x\boldsymbol{\rho}_n)$. Subsequent use of Eqs. [3], [4], [6] results in

$$\begin{aligned}\delta(x, y, n) &= 100[1 - \mathrm{Tr}(I_x\boldsymbol{\rho}_n)]\\ &= 100\sin^2[\Theta_{\mathrm{eff}}(x, y)]\\ &\quad\times\{1 - \cos[2n\Phi_{\mathrm{eff}}(x, y)]\}. \qquad [10]\end{aligned}$$

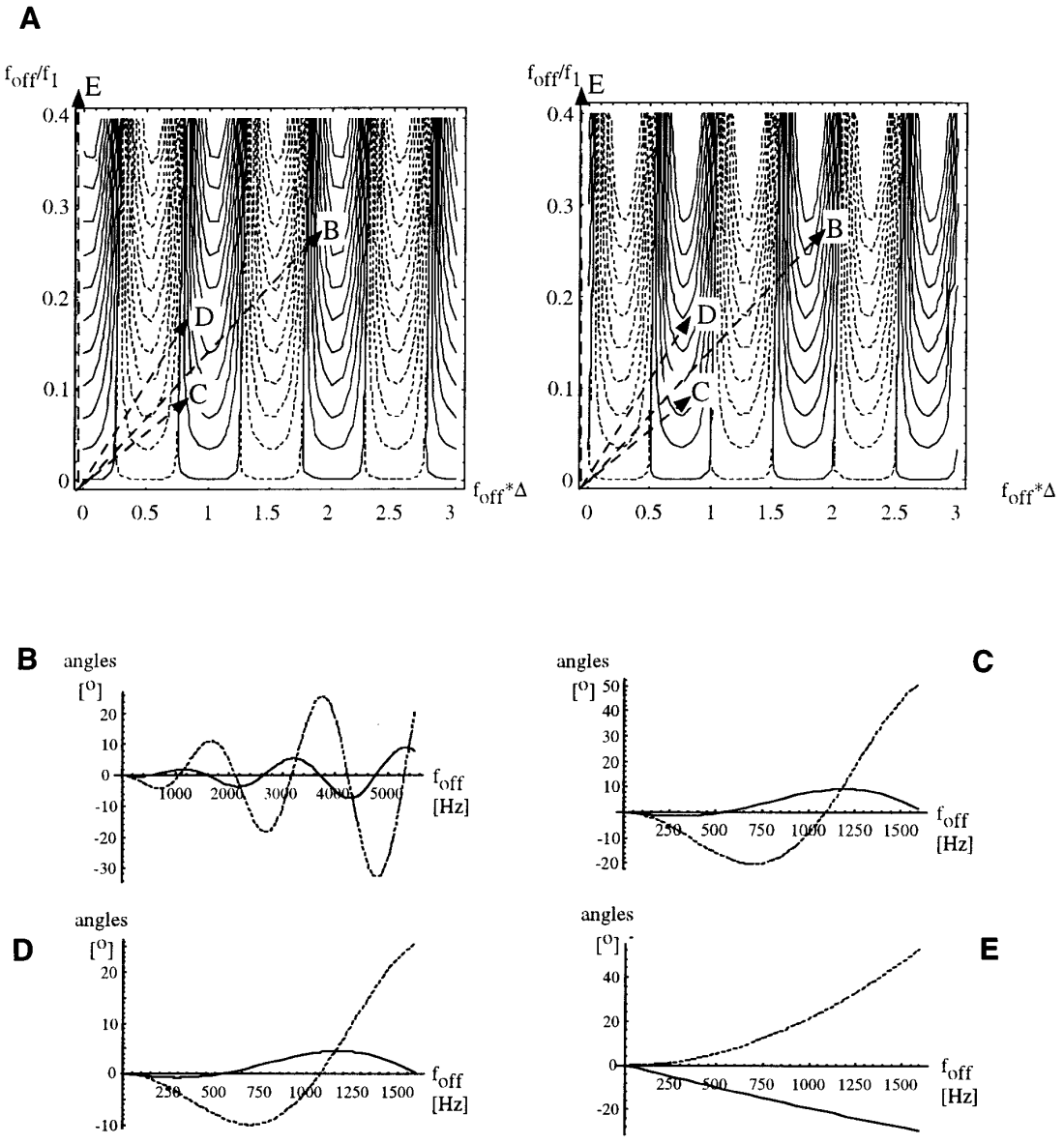

FIG. 2. (A) Dependence of the tilt angle $\Theta_{eff}(x, y)$ (left) and the precession angle $\Phi_{eff}(x, y)$ (right) on the normalized frequency parameters defined in Eq. [9]. Solid contours correspond to counterclockwise rotations at 4° intervals. Dotted lines show clockwise rotations at the same interval. (B–E) Offset dependencies for a set of B_1 and Δ parameters typical of biomolecular relaxation experiments at the equivalent of 750 MHz proton frequency and a delay Δ of 475 μs. Solid lines represent precession angles Φ_{eff}, dotted lines show tilt angles Θ_{eff}. (B) Representative parameters for ^{13}C relaxation measurements on nucleic acids: sweep width 11.5 kHz (9.5 kHz at 600 MHz), 180° pulse length of 15 μs. (C) ^{15}N relaxation measurements on a protein backbone: sweep width 3.2 kHz (2.5 kHz at 600 MHz), 180° pulse length of 70 μs. (D) Same as (C), but with a 180° pulse length of 35 μs. (E) Profile for a continuous spin lock of 3 kHz.

The factor of 100 normalizes the systematic error of the measurement as a percentage. The amplitude of the oscillating contribution that determines the size of the introduced error can be calculated from

$$\delta_{worst}(x, y) = 2\{100 \sin^2[\Theta_{eff}(x, y)]\}. \qquad [11]$$

The resulting dependence of $\delta_{worst}(x, y)$ on the normalized parameters is given in Fig. 3.

An interesting feature of the equations is that there must be settings of the experimental parameters that give the result $\Phi_{eff}(f_{off}, f_1, \Delta) = \pi m$ ($m = 1, 2 \ldots$), or $\Theta_{eff}(x, y) = 0$. This situation corresponds to magnetization precessing exactly m times around the effective rotation axis or an axis aligned perfectly along the initial magnetization respectively. In both cases, no oscillatory component is seen with increasing numbers of repetitions, and decay constants measured at these offsets will lack any systematic error. Since

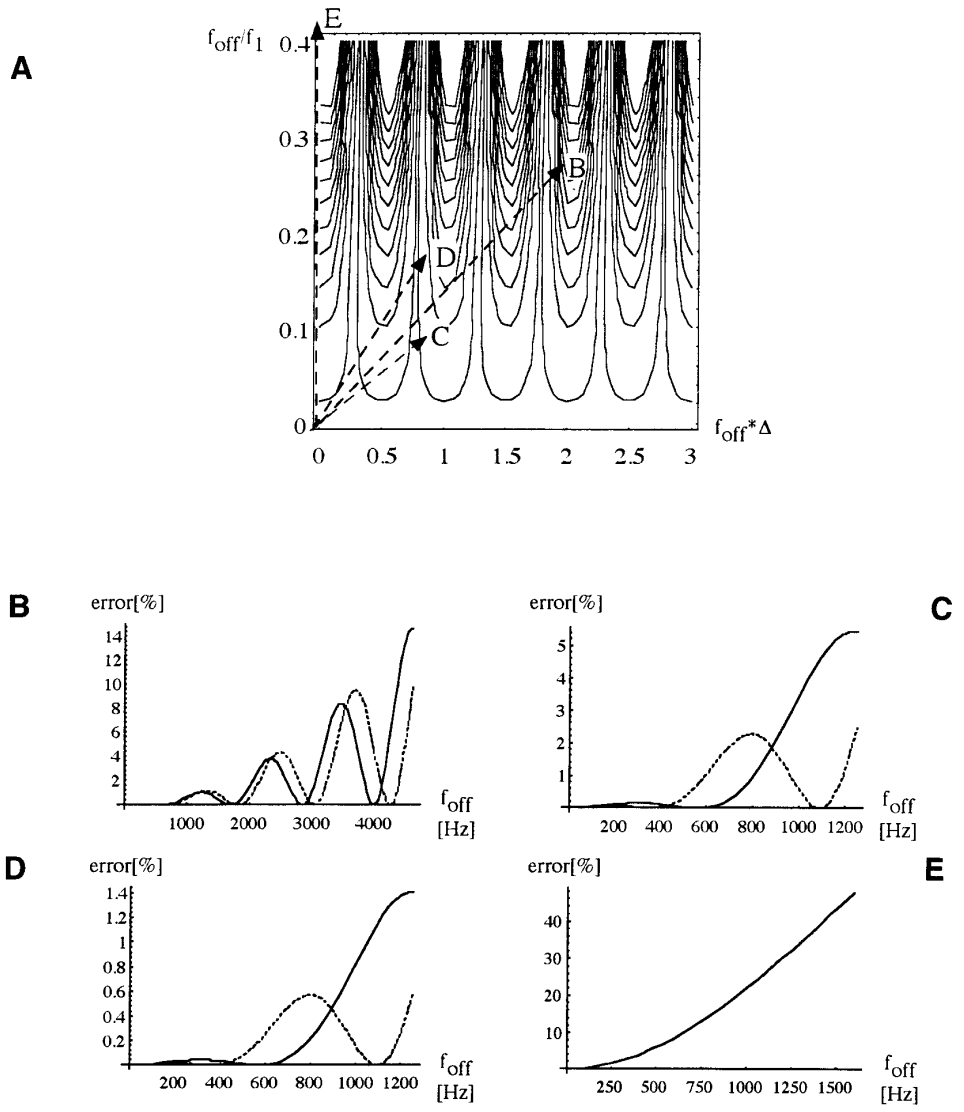

FIG. 3. (A) Dependence of the maximum amplitude error δ_{worst} given in Eq. [11] on the normalized parameters defined in Eq. [9]. Contours correspond to errors of 0.1, 2, 4, 6, 8, 10, 12, 14, 16, 18, and 20%. (B–E) Amplitude errors corresponding to the conditions of Figs. 2B–2E at 600 MHz proton frequency. Solid lines refer to settings of Δ that maximize errors ($\equiv\Delta_{worst}$), while dotted lines indicate settings Δ_{best} that minimize the maximum error. Values found in the proximity of the initial setting $\Delta = 475$ μs are: (B) $\Delta_{worst} = 437$ μs, $\Delta_{best} = 457$ μs, (C) $\Delta_{worst} = 460$ μs, $\Delta_{best} = 705$ μs, (D) $\Delta_{worst} = 420$ μs, $\Delta_{best} = 447$ μs. Settings found for 750 MHz proton frequency are: (B) $\Delta_{worst} = 420$ μs, $\Delta_{best} = 447$ μs. (C) $\Delta_{worst} = 360$ μs, $\Delta_{best} = 550$ μs, (D) $\Delta_{worst} = 355$ μs, $\Delta_{best} = 543$ μs.

these conditions only hold for ''singular'' offset frequencies (dependent on the experimental parameters of the sequence), proper selection of the CPMG parameters should not be influenced by this property.

MATERIALS AND METHODS

NMR experiments were performed on a Bruker DMX-600 spectrometer equipped with a three-axis triple-resonance probehead. The reference sample was 600 μl of 10% H_2O/90% D_2O to provide a single resonance line with reduced radiation damping. Proton T_2 relaxation curves for this sample were measured at different offset frequencies. To mimic a situation comparable to that found with the use of a large-diameter or triple-resonance probehead to measure ^{15}N relaxation in proteins, the length of the 180° pulse was set to 100 μs and the interpulse delay Δ was set to 475 μs (*9*). To minimize offset effects of the initial excitation, the single 90° pulse length was set to 13 μs. To prevent the detection of magnetization caused by T_1 relaxation during the CPMG sequence, a two-step $(x, -x)$ phase cycle of the 90° pulse and the receiver was employed. A 5 s relaxation delay was

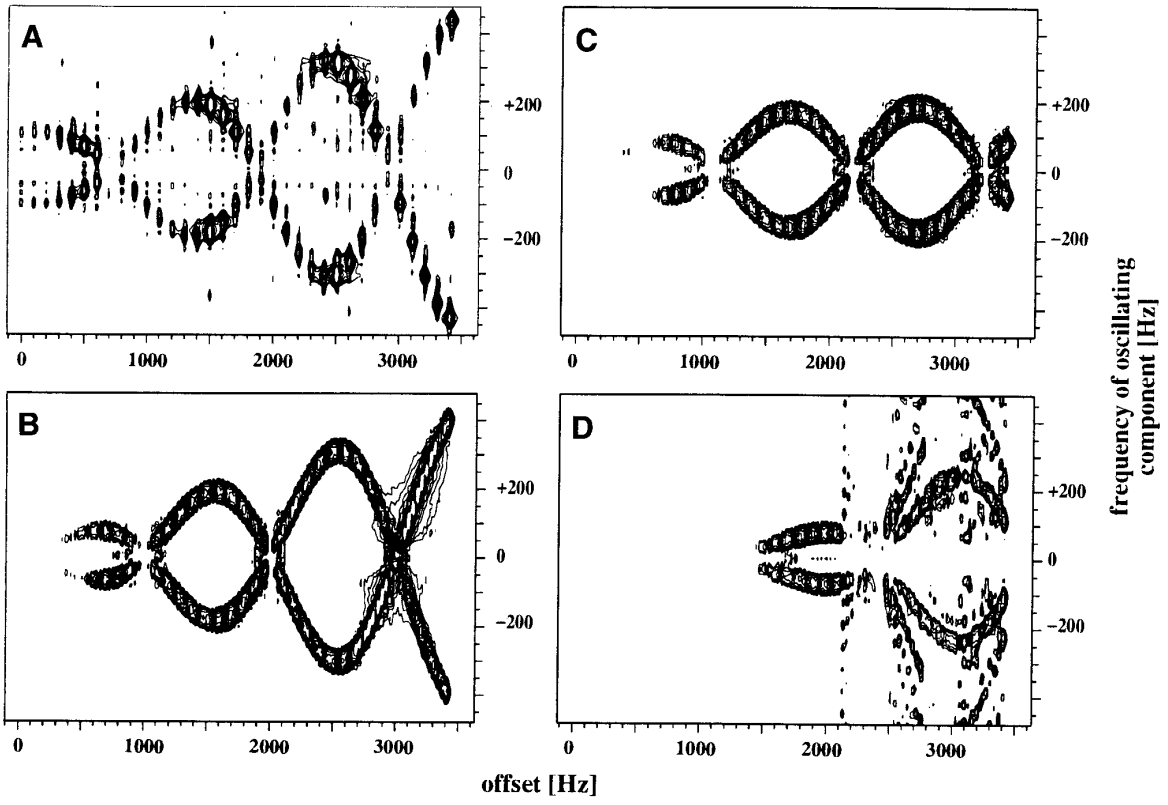

FIG. 4. Two-dimensional representation of experimental and simulated refocusing spectra. The *x* axis corresponds to the resonance offset. The sweep width shown along f_1 is 925 Hz, given by $[2[(2\Delta + T_{180})]^{-1}$. (A) Experimental result with parameters as described under Materials and Methods. (B) Simulation corresponding to (A). (C) Simulation for a $90^\circ_x 180^\circ_y 90^\circ_x$ composite pulse. (D) Simulated profile using a $90^\circ_x 270^\circ_y 90^\circ_x$ pulse.

included to ensure adequate equilibration between scans. The off-resonance profile of the sequence was measured in 35 equidistant steps ranging from 0 to 3400 Hz, with the detected signals of all steps added in the spectrometer ADC prior to storage on disc. This profile was recorded for all repetitions up to 40 times the basic CPMG block (corresponding to 80 times the reduced block). Two scans were summed for each frequency step by performing the phase cycling described, resulting in a total measurement time of 4 h. Along the acquisition dimension, 4K complex data points were recorded using the Bruker simultaneous quadrature acquisition mode, yielding a raw data matrix of 40 × 8K points.

Prior to Fourier transformation, a Gaussian window was applied in the t_2 dimension. To clarify the offset-dependent oscillatory behavior of the systematic error along the incremented length of the CPMG sequence, the data were treated as complex t_1 points of a complex Fourier transform after apodization with a $\pi/3$-shifted cosine-squared window. To suppress the large central line that corresponds to the nonoscillating component of the refocused magnetization, a baseline correction along t_1 was employed on the time-domain data (*21*). The size of the final ''refocusing spectrum'' (Fig. 4) was 128 × 8K data points. For quantitative analysis the traces shown in Fig. 5 were processed without recourse to baseline correction. As the data are not recorded in quadrature along t_1, all spectra are shown in absolute-value mode. Identical experiments were performed with composite $90^\circ_x 180^\circ_y 90^\circ_x$ (*22*) and $90^\circ_x 270^\circ_y 90^\circ_x$ (*23*) pulses in place of the simple 180° pulse. To ensure that the duration of the CPMG sequences using these composite pulses was the same as the original, the delay Δ was adjusted to 425 and 406 μs, respectively (data not shown).

Numerical calculations based on the Bloch equations were performed using in-house software running on an SGI Indigo^2 workstation. The program simulated serial files of the sizes described above composed of excitation profiles with an artificially introduced linewidth of 2.0 Hz. The offset behavior was calculated at one-hundred 34 Hz intervals with a range of CPMG block repetitions according to experimental parameters. All serial files were processed using Bruker XWIN-NMR software. The Mathematica calculations of the quaternion formalism were performed on an Apple Power Macintosh 7200/90 personal computer.

RESULTS AND DISCUSSION

Consideration of the systematic errors caused by CPMG off-resonance effects can be subdivided into four questions:

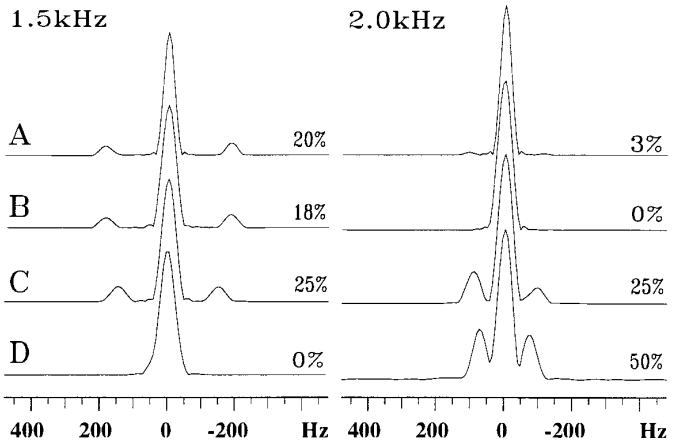

FIG. 5. Cross sections from nonbaseline corrected refocusing spectra. Traces were taken from Fig. 4 at offset intersections of 1.5 kHz (left) and 2.0 kHz (right) respectively. (A) Experimental result of the sequence Δ—180°_x—Δ. (B) Numerical simulation corresponding to (A). (C) Simulation using the sequence Δ'—$90^\circ_x 180^\circ_y 90^\circ_x$—$\Delta'$. (D) Simulation with Δ''—$90^\circ_x 270^\circ_y 90^\circ_x$—$\Delta''$. The asymmetry apparent in 2 kHz row (C) is introduced by baseline distortion from a neighboring line.

(1) What is the size and significance of any errors that these effects introduce into measured peak amplitudes? (2) Can systematic errors be minimized with B_1 and Δ settings or other approaches? (3) How do peak-amplitude errors transfer to errors in T_2 values obtained by curve fitting? (4) What effect do T_2 errors have on the analysis of mobility using the Lipari–Szabo formalism?

Quantification of Systematic Errors

The dependence of the tilt angle $\Theta_{\text{eff}}(x, y)$ and the precession angle $\Phi_{\text{eff}}(x, y)$ upon experimental parameters is summarized in Fig. 2, where it can be seen that conditions typical of heteronuclear T_2 measurements on biomolecules yield significant deviations from ideal behavior, particularly for Θ_{eff} where values up to 50° are observed toward the spectral edge. The influence on peak amplitudes is summarized in Fig. 3, where settings of the delay Δ that produce minimum and maximum errors in $\delta_{\text{worst}}(x, y)$ are compared. Not surprisingly, the greatest deviations are found for conditions corresponding to ^{13}C measurements, where spectral widths are greater.

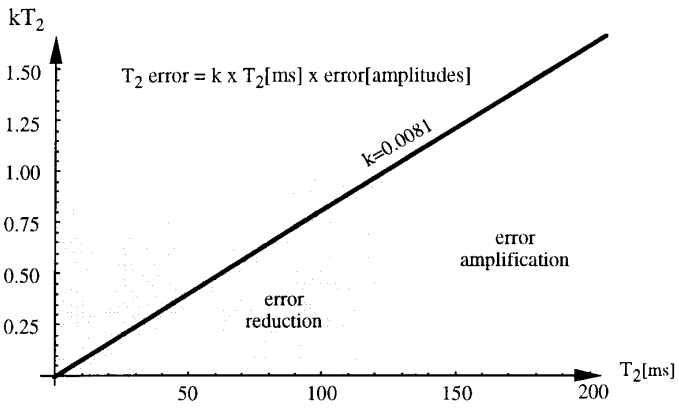

FIG. 6. Transformation of peak amplitude errors to T_2 fit errors. The figure was generated with artificial data given by $A^{\text{perfect}} = \exp(-T/T_2)$ with T = 10, 20, 40, 60, 80, 100, 200, and 300 ms. Systematic errors of up to 30% were subtracted from all points. The value of constant k depends on the choice of measurement timepoints. The figure can be read as follows: if an error of less than 5% is expected in the measured amplitude data then for a fitted T_2 value of 100 ms, the error is given by $0.0081 \times 100 \times 5 = 4.1\%$.

TABLE 1
Errors in Fitted T_2 Values for Representative Hardware Configurations

Proton frequency (MHz)	180° pulse length (μs)	Spectral width	T_2 error	
			Δ_{best} (%)	Δ_{worst} (%)
750	30	11.6 kHz, ^{13}C	< -16	< -22
750	70	3.2 kHz, ^{15}N	< -4	< -9
600	30	9.6 kHz, ^{13}C	< -10	< -15
600	35	2.5 kHz, ^{15}N	< -1	< -2
600	70	2.5 kHz, ^{15}N	< -3	< -6

To better observe the effect of precession about the tilted reference frame given in Eq. [8], data were Fourier transformed not only along the acquisition dimension but also with respect to the number of repetitions of the CPMG sequence. A comparison of experimental and simulated refocussing spectra is shown in Fig. 4A and 4B, where good agreement is apparent. The sidebands in Fig. 4 report on the oscillating contribution superimposed upon the exponentially damped magnetization, their offsets and amplitudes corresponding to the frequencies and magnitudes of these oscillations, respectively. Offset frequencies of perfect refocusing are evident at the centers of sideband crossing points. The relative sizes of the sidebands are indicated in Fig. 5, where cross sections through refocusing spectra at offsets of 1.5 kHz (left panel) and 2.0 kHz (right panel) are shown. Oscillating components may account for 0–50% of the nonoscillating signal intensity.

Minimization of Peak Amplitude Errors

The performance of the CPMG sequence with regard to the maximum systematic error can be improved by using Eqs. [8] and [11] to calculate the dependence of the error on the normalized parameters given by Eq. [9]. Inspection of Fig. 3 shows that increasing the field strength of the 180° pulse improves the refocusing performance of the sequence, as may be expected. The delay Δ can then be varied provided that the condition $T_{180} \ll \Delta \ll 1/J$ is fulfilled. The left-hand side of this condition ensures that a mixture of T_2 and T_1 relaxation behaviors is not measured, while the right-hand side is necessary to remove effects caused by relaxation of

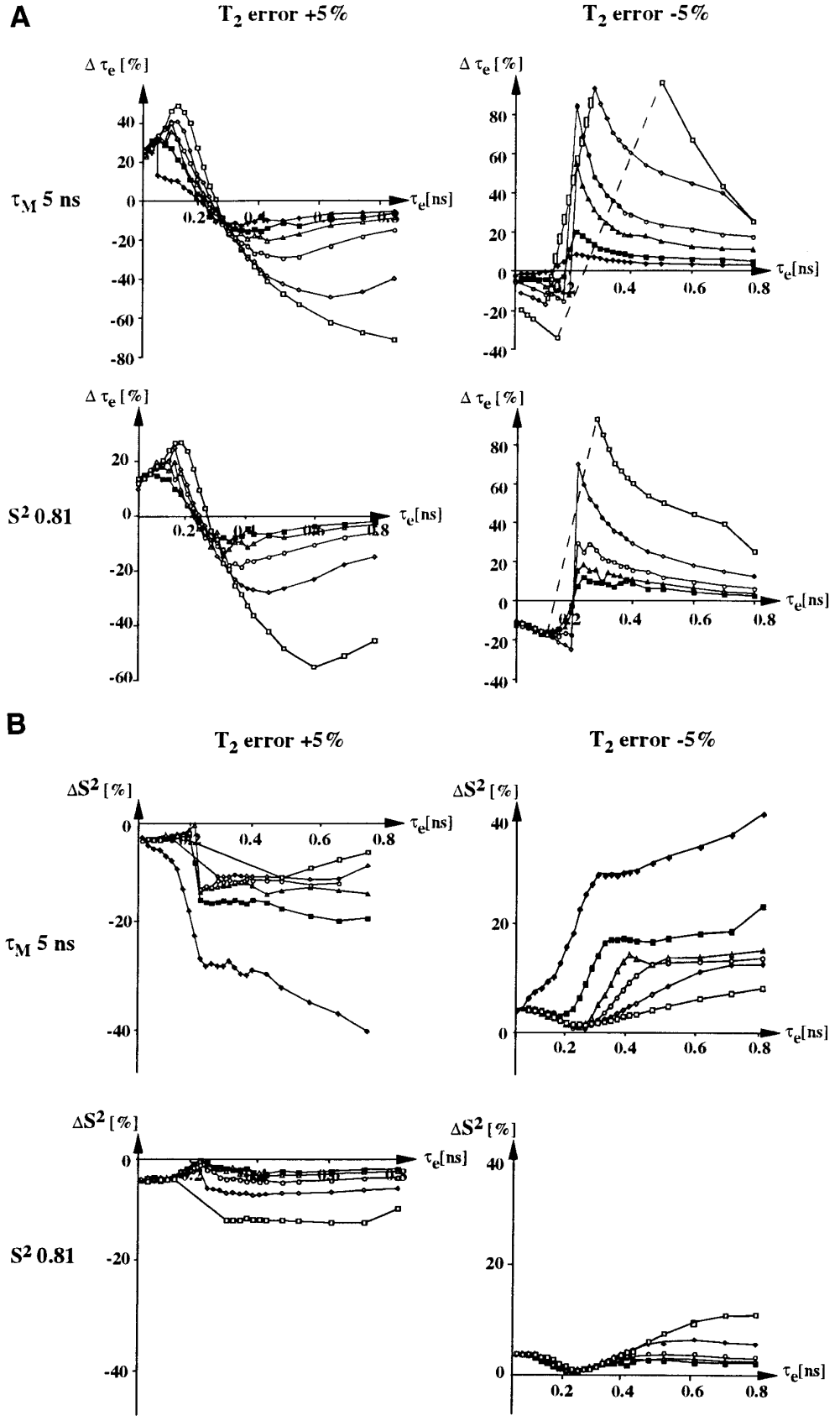
A
T2 error +5%
T2 error -5%
Δ τe [%]
τM 5 ns
S2 0.81
τe[ns]
B
ΔS2 [%]

TABLE 2
Errors in Lipari–Szabo Mobility Parameters Caused by T_2 Errors of ±5%

τ_M (ns), S^2	Range of error in S^2 (%) for +5%, −5% error in T_2	Range of error in τ_e (%) for +5%, −5% error in T_2
5, 0.81	[0, +8], [−8, 0]	[+27, −55], [−18, +92]
5, 0.64	[0, 9], [−10, 0]	[+17, −32], [−15, +85]
5, 0.25	[0, +16], [0, −14]	[+5, −13], [−4, +20]
10, 0.81	**[0, +5], [0, −5]**	**[+25, −28], [−25, +70]**
10, 0.64	**[0, +6], [−6, 0]**	**[+9, −18], [−12, +31]**
10, 0.25	**[0, +8], [−12, 0]**	**[+3, −12], [−5, +6]**
15, 0.81	[0, +3], [−3, 0]	[+20, −19], [−18, +30]
15, 0.64	[0, +5], [−6, 0]	[+9, −11], [−9, +14]
15, 0.25	[0, +7], [−9, 0]	[+3, −3], [−4, +3]

Note. Parameters corresponding to a molecule of approximately 14 kDa are in boldface.

a scalar-coupled spin. Setting the value of Δ within this range determines the offset dependence and the maximum size of the introduced error.

Because the oscillatory behavior is strongly dependent on the value of Δ, it can be appreciated that there are settings of Δ that minimize (or respectively maximize) the systematic error. Careful setting of Δ can halve the error introduced in some cases—this is shown in Figs. 3B–3D where maximum peak amplitude errors for the best and worst settings of Δ are compared. The off-resonance profile of a continuous spin-lock pulse of 3.0 kHz is shown in Fig. 3E for comparison. A large oscillating component predicted for this technique (not shown) is not observed experimentally as the inhomogeneity of the applied B_1 field serves to defocus the component not aligned parallel to the effective field within a few milliseconds, leaving the component spin-locked along the effective field to decay with the mixture of T_1 and $T_{1\rho}$ relaxation times as given in the literature (*13*). Provided that only time points longer than the dephasing period are taken, this approach is one way to circumvent the introduction of the systematic errors discussed here. A simple approach that may prove effective in some instances is to record T_2^* via free precession (*24*), where the contribution of static field inhomogeneity is not significant in comparison to biomolecular linewidths.

Composite pulse schemes and more elaborate phase cycling (e.g., Δ—180°_x—Δ—Δ—180°_x—Δ—Δ—180°_x—Δ—Δ—180°_x—Δ) can provide some assistance, but do not remove much systematic error. Our simulated and experimental results of Figs. 4 and 5 show that the sidebands cannot be substantially eliminated over a wide frequency range by these methods. Instead, only a modification of the offset dependence is observed.

Transfer of Errors to Apparent Decay Constants

The effect of signal amplitude errors defined in Eq. [11] on the fit of experimental time-series data to a T_2 decay constant can have a variable outcome depending on a number of parameters. We have estimated this contribution with the following procedure. A set of N error-free amplitudes is defined for a perfect T_2 fit $\{A_i^{\text{perfect}} = \exp(-T_i/T_2)\}$, where the total lengths of the CPMG sequences employed are given by $\{T_i\}$. When considering the behavior at any distinct offset frequency, two limiting sets of peak amplitudes can be determined. The first

$$\{A_i\}^{\min}(T_2, \delta_{\text{worst}}) = \{A_1^{\text{perfect}}(1 - \delta_{\text{worst}}), \ldots, A_{N/2}^{\text{perfect}}(1 - \delta_{\text{worst}}), A_{N/2+1}^{\text{perfect}}, \ldots, A_N^{\text{perfect}}\}$$

results in the most underestimated T_2 value $[\equiv T_2^{\min}(T_2, \delta_{\text{worst}})]$ upon fitting. These time series points produce a slower decay than is actually experienced by the spin. Correspondingly, the set $\{A_i\}^{\max}$ that produces the most overestimated value $T_2^{\max}(T_2, \delta_{\text{worst}})$ is given by

$$\{A_i\}^{\max}(T_2, \delta_{\text{worst}}) = \{A_1^{\text{perfect}}, \ldots, A_{N/2}^{\text{perfect}}, A_{N/2+1}^{\text{perfect}}(1 - \delta_{\text{worst}}), \ldots, A_N^{\text{perfect}}(1 - \delta_{\text{worst}})\}.$$

The value $\delta T_2(T_2, \delta_{\text{worst}}) \equiv T_2^{\max}(T_2, \delta_{\text{worst}}) - T_2^{\min}(T_2, \delta_{\text{worst}})$ defines the range of T_2 values that may be observed in practice. This range is dependent on the size of the systematic error δ_{worst}, the ''correct'' decay constant T_2, and the choice of the time series set $\{T_i\}$. It is not clear whether this maximum possible range of errors will actually be experienced by any spin, but this is at least theoretically possible. To answer this question in any particular instance, a detailed analysis using the theory outlined here is needed. The only general statement that can be made is that all errors found

FIG. 7. Error dependence of motional parameters. (A) Behavior of the local correlation time τ_e for T_2 errors of +5% (left) and −5% (right). In the top row, the global correlation time τ_m is set to 5 ns while the order parameter S^2 takes on values of 0.9 (□), 0.81 (◇), 0.64 (○), 0.49 (△), 0.25 (■), and 0.1 (◆). In the second row, S^2 is fixed at 0.81 for a range of global correlation time τ_m values of 5 ns (□), 10 ns (◇), 15 ns (○), 20 ns (△), and 25 ns (■). (B) Behavior of the order parameter S^2 under the same conditions as (A). All data points where calculated with a random search algorithm (30,000 trials), minimizing the deviation of the initial T_1, T_2, NOE values from their theoretical values by screening the two-dimensional space (τ_e, S^2) in the relevant range. Note: missing data points (connected with dashed lines) correspond to initial settings where the fit failed to converge.

in the decay constants will lie within the range encompassed by $\delta T_2(T_2, \delta_{worst})$.

To determine $\delta T_2(T_2, \delta_{worst})$, sets of amplitudes $\{A_i\}^{min}(T_2, \delta_{worst})$ and $\{A_i\}^{max}(T_2, \delta_{worst})$ consisting of eight data points each (corresponding to time points $\{T_i\}$ given in the legend to Fig. 6) were constructed for different initial settings of T_2 and δ_{worst}. Using a standard least-squares fitting procedure, deviations from the initial T_2 values were then calculated. The results summarized in Fig. 6 can be parameterized by the equation

$$\delta T_2(T_2, \delta_{worst}) = k(\{T_i\})T_2\delta_{worst}. \quad [12]$$

For long T_2 values, the systematic error in the peak amplitudes is ''amplified'' by the fitting routine. This can be understood by considering a signal of no decay, where the introduction of an arbitrarily small systematic error corresponds to a large error in the fit. Correspondingly, errors are reduced at short T_2 values. These results indicate that the systematic error is expected to have a more serious effect on those signals from the more flexible parts of the molecule under investigation. The constant $k(\{T_i\})$ reflecting the transfer of the error is dependent on the set of time points $\{T_i\}$. It should be mentioned that the mathematical treatment of a systematic nonstatistical error is different to that of a statistical error. In this case, a statistical error would have the same absolute size for all amplitudes, whereas the absolute size of the error discussed here is proportional to the size of the value measured. As shown in Table 1, attempts to minimize T_2 errors by optimal setting of Δ are not highly successful, yielding a factor of two improvement in the best cases.

Error Transfer to Motional Parameters

The final step in analyzing the effect of the systematic error in signal amplitudes corresponds to the transfer of errors in fitted T_2 values to errors in modeled motional parameters. From the above, it is clear that care should be taken to interpret data when additional ''local'' parameters are included in motional descriptions. The Lipari–Szabo approach without additional correction (*4*) is treated as an example, where the procedure applied is basically the same as that outlined for the transfer from peak amplitudes to T_2 values. The dependence of derived τ_e and S^2 values on T_2 was calculated by introducing a reasonably conservative error of $\pm 5\%$ into a set of T_2 values applied to the fit routine. As indicated in Table 1, there are occasions when much larger errors may be encountered. Fits were performed for a set of fixed τ_m values ranging from 5 to 25 ns, which correspond to values typical of biomolecular studies. Figure 7 depicts the parameter dependence of errors in τ_e (Fig. 7A) and S^2 (Fig. 7B) on τ_M, S^2, and the sign of the T_2 error, while representative cases for macromolecules of three different sizes are summarized in Table 2. It is evident that error transfer is strongly dependent on all parameter settings. For the local correlation time τ_e, the following general trends are apparent: (1a) The error in τ_e increases for increasing τ_e values, (2a) the error decreases as S^2 decreases (i.e., as motions become less restricted), and (3a) errors decrease with increasing τ_M. Even for the moderate T_2 error examined here, inaccuracies in the value of the local correlation time of up to 100% can occur.

Errors in the fit of S^2 were somewhat smaller than those of τ_e under the conditions examined, reaching 50% in the worst cases. For S^2, the trends (1a–3a) must be modified as follows: (1b) The error in S^2 increases with increasing τ_e, (2b) the error in S^2 decreases with decreasing motional restriction, and (3b) the opposite holds true for increasing τ_M. It is expected that larger T_2 errors will produce larger deviations in S^2. For certain motional regimes, the introduction of an erroneous T_2 caused nonconvergence of the search algorithm.

It is clear that the general trends outlined above hold true for T_2 errors of any origin—systematic errors need not be the major cause of T_2 deviations. In unfavorable instances, differences in motional properties derived from relaxation analysis are expected to lie in the range of the systematic errors for certain spins, a situation that will worsen at higher spectrometer operating frequencies. Overinterpretation of the experimental data can be avoided by error analysis using the worst case scenario outlined above. If motional analysis using additional local parameters is desirable and is thought justified, application of Eqs. [8] and [10] to calculate the systematic error in each measured T_2 time point is advisable. In theory, it should be possible to perform a real back correction of the amplitudes in CPMG spectra via nonlinear phase correction (removing the antiphase contribution) and amplitude rescaling (compensating for the loss of transverse magnetisation) with respect to f_1. However, this procedure is cumbersome, and effects caused by slightly overlapping signals (see Fig. 6 row C) and the introduction of f_1-dependent noise may introduce statistical errors in the data that could obviate the desired improvement.

CONCLUSIONS

We have shown that CPMG pulse sequence parameters commonly used in T_2 relaxation experiments on biomolecules can often introduce systematic errors of 5–25% into measured peak amplitudes (Figs. 3, 5). Theoretical and experimental results show that a critical feature of these errors is their nonlinearity with respect to signal offset (Fig. 4). Imperfections in measured peak amplitudes propagate through to T_2 fitting procedures, yielding potential errors of a similar magnitude (Fig. 6, Table 1). Errors can further propagate to motional modeling using the Lipari–Szabo formalism, producing errors of up to 100% in τ_e and 50% in

S^2 values under reasonably conservative conditions. The major trap lies in the fact that misinterpretation of mobilities can be restricted to distinct offset frequencies. None of the methods normally used to improve the performance of a pulse sequence (composite pulses, shaped pulses, iterative phase cycling) solves the off-resonance problem entirely satisfactorily. The shortest viable 180° pulse length should be employed in CPMG experiments, and optimal setting of the delay Δ helps to reduce the size of the oscillating contribution to some extent. The spin-lock technique proposed by Peng *et al.* (*12*, *13*) solves the off-resonance problem satisfactorily if only data points that ensure defocusing of unwanted signal contributions are used, but requires its own correction for off-resonance effects.

ACKNOWLEDGMENTS

This work was supported by the Australian Research Council. We thank G. W. Vuister and M. Tessari for inspiring discussions and final reading of the manuscript.

REFERENCES

1. L. E. Kay, D. A. Torchia, and A. Bax, *Biochemistry* **28,** 8972 (1989).
2. N. R. Nirmala and G. Wagner, *J. Am. Chem. Soc.* **110,** 7557 (1988).
3. P. G. Schmidt, H. Sierzputowska-Gracz, and P. F. Angris, *Biochemistry* **26,** 8529 (1987).
4. G. Lipari and A. Szabo, *J. Am. Chem. Soc.* **104,** 4546 (1982).
5. G. M. Clore, A. Szabo, A. Bax, L. E. Kay, P. C. Driscoll, and A. M. Gronenborn, *J. Am. Chem. Soc.* **112,** 4989 (1990).
6. G. M. Clore, P. C. Driscoll, P. T. Wingfield, and A. M. Gronenborn, *Biochemistry* **29,** 7387 (1990).
7. T. Zink, A. Ross, K. Lüers, C. Cieslar, R. Rudolph, and T. A. Holak, *Biochemistry* **33,** 8453 (1994).
8. Z. Zheng, J. Czaplicki, and O. Jardetzky, *Biochemistry* **34,** 5212 (1995).
9. L. K. Nicholson, L. E. Kay, D. M. Baldisseri, J. Arango, P. E. Young, A. Bax, and D. A. Torchia, *Biochemistry* **31,** 5253 (1992).
10. S. Meiboom and D. Gill, *Rev. Sci. Instrum.* **29,** 688 (1958).
11. J. Simbrunner and R. Stollberger, *J. Magn. Reson. B.* **109,** 301 (1995).
12. J. W. Peng, V. Thanabal, and G. Wagner, *J. Magn. Reson.* **95,** 421 (1991).
13. J. W. Peng, V. Thanabal, and G. Wagner, *J. Magn. Reson.* **94,** 82 (1991).
14. L. E. Kay, L. K. Nicholson, F. Delaglio, A. Bax, and D. A. Torchia, *J. Magn. Reson.* **97,** 359 (1992).
15. F. Bloch, *Phys. Rev.* **70,** 460 (1946).
16. O. W. Sørensen, G. W. Eich, M. H. Levitt, G. Bodenhausen, and R. R. Ernst, *Prog. NMR Spectrosc.* **16,** 163 (1983).
17. R. R. Ernst, G. Bodenhausen, and A. Wokaun, ''Principles of Nuclear Magnetic Resonance in One and Two Dimensions,'' p. 120, Clarendon Press, Oxford, 1992.
18. J. P. Elliott and P. G. Dawber, ''Symmetry in Physics,'' Vol. 2, p. 480, Macmillan, London, 1979.
19. C. Counsell, M. H. Levitt, and R. R. Ernst, *J. Magn. Reson.* **63,** 133 (1985).
20. S. Wolfram, ''Mathematica A System for Doing Mathematics by Computer,'' 2nd ed. Addison-Wesley, Redwood City, California, 1991.
21. D. Marion, M. Ikura, and A. Bax, *J. Magn. Reson.* **84,** 425 (1989).
22. M. H. Levitt, and R. Freeman, *J. Magn. Reson.* **43,** 65 (1982).
23. M. H. Levitt, and R. Freeman, *J. Magn. Reson.* **33,** 473 (1979).
24. G. C. King, J. W. Harper, and Z. Xi, *Meth. Enzymol.* **261,** 436 (1995).